Am J Transl Res 2025;17(6):4159-4174
www.ajtr.org /ISSN:1943-8141/AJTR0161059

Original Article

Recombinant human bone morphogenetic protein-2 (rhBMP-2) induced macrophage biphasic polarization regulated by dexamethasone in vivo

Aikebaier Aixirefu[1], Yang Liu[2,3], Jing Wang[2,3]

[1]Clinical Department of Orthopedics, Ya'an Traditional Chinese Medicine Hospital, Ya'an 625000, Sichuan, China; [2]The State Key Laboratory of Bioreactor Engineering, East China University of Science and Technology, Shanghai 200237, China; [3]Key Laboratory for Ultrafine Materials of Ministry of Education, East China University of Science and Technology, Shanghai 200237, China

Received October 10, 2024; Accepted May 11, 2025; Epub June 15, 2025; Published June 30, 2025

Abstract: Objectives: To evaluate macrophage polarization dynamics in vivo after implantation of recombinant human bone morphogenetic protein-2 (rhBMP-2) incorporated biomaterials, with a focus on dose-dependent effects and polarization modulation strategies. Methods: A murine dorsal subcutaneous implantation model was utilized to analyze macrophage responses to varying concentrations of rhBMP-2-loaded biomaterials with or without dexamethasone (Dex). Polarization patterns were assessed through phenotypic characterization and cytokine expression profiling. Results: Elevated rhBMP-2 concentrations amplified macrophage polarization activities, and concurrent activation of M1 and M2 polarization was observed accompanied by enhanced expression of both pro-inflammatory (M1-associated) and anti-inflammatory (M2-associated) cytokines. Dexamethasone co-administration effectively attenuated pro-inflammatory polarization patterns induced by high-dose rhBMP-2 implants while preserving regenerative cytokine expression. Conclusions: Optimized rhBMP-2 dosage facilitates a balanced macrophage polarization state, creating a pro-regenerative microenvironment through coordinated inflammatory resolution and tissue remodeling signals. For clinical applications requiring high rhBMP-2 doses, concurrent short-term anti-inflammatory therapy (e.g., dexamethasone) is recommended to mitigate excessive M1 polarization without compromising osteoinductive capacity.

Keywords: Macrophage, polarization, BMP-2, bio-material, dexamethasone

Introduction

Inflammation represents a dynamic biological phenomenon characterized by intricate cellular interactions and coordinated mediator cascades. Optimal inflammatory activation has been experimentally validated as a critical regulatory mechanism for initiating physiological tissue repair pathways [1, 2]. Paradoxically, both insufficient cytokine signaling and hyperactive immune responses may induce pathological alterations in molecular signaling networks, ultimately leading to compromised regenerative outcomes [3-5].

Biomaterial implantation triggers a dynamic immune cascade characterized by macrophage activation and cytokine storm initiation, constituting the primary host defense mechanism against exogenous substances [6, 7]. This biological phenomenon, clinically termed foreign body reaction, manifests as spatiotemporal regulation of leukocyte infiltration and proteolytic cascades at implant sites.

It is well-established that monocytes-derived macrophages constitute the primary cellular component at bio-material interfaces during both inflammatory and regenerative phases [8]. As pivotal regulators of aseptic inflammatory cascades and tissue remodeling outcomes, macrophages critically influence host responses toward implanted devices. Upon migration, these cells engage in dynamic material interrogation while orchestrating foreign body reactions through coordinated release of cytokines,

https://doi.org/10.62347/UGHK3747

growth mediators, and chemotactic signals [9, 10]. Contemporary research demonstrates macrophages' exceptional phenotypic adaptability, enabling functional specialization through environment-driven polarization into distinct subpopulations [11-15, 20]. This plasticity manifests in two principal activation states: The classically activated M1 phenotype exhibits pro-inflammatory characteristics through elevated secretion of tumor necrosis factor (TNF-α), interleukin-6 (IL-6), and interleukin-1β (IL-β), mediating antimicrobial defense and acute inflammatory processes [16-19]. Conversely, the alternatively activated M2 phenotype promotes resolution phases by releasing interleukin-10 (IL-10), transforming growth factor-β (TGF-β), and interleukin-1RA (IL-1RA), thereby facilitating regenerative processes and extracellular matrix reconstruction [21]. Temporal analysis reveals an immunological progression pattern: M1 macrophages predominantly occupy implantation sites during acute phases (1-5 days post-operation), whereas M2 populations gradually dominate during subacute stages (4-10 days), despite their concurrent presence at initial time points [20-22]. This chronological dominance shift underscores macrophages dual regulatory roles in balancing inflammatory clearance and tissue restoration.

As a clinically recognized osteoinductive cytokine, bone morphogenetic protein-2 (BMP-2) has obtained United States Food and Drug Administration approval for spinal fusion and fracture repair procedures, demonstrating significant therapeutic value in bone regeneration. Although achieving extensive clinical adoption, its administration has revealed dose-dependent complications including inflammatory infiltration and edema formation [23, 24]. These manifestations may progress to cervical swelling with airway compression risks, particularly in unapproved surgical scenarios requiring high-dose applications. Current research efforts have been focused on characterizing BMP-2's pro-inflammatory properties through preclinical models. In the study conducted by Lee *et al.*, BMP-2 implantation induced soft-tissue swelling in the surrounding tissues along with sterile seroma and hematoma formation [25]. Despite these phenomenological observations, the cellular mechanism mediating such immune activation remain insufficiently elucidated.

In addition, extensive studies focused on immune response initiated by bone morphogenetic protein-7 (BMP-7), the other members of the bone morphogenetic proteins. For instance, Rocher *et al.* found that BMP-7 polarized monocytes into M2 macrophages and enhanced anti-inflammatory cytokine expression *in vitro* [26]. Studies by Dinender *et al.* reported that BMP-7 possessed novel therapeutic potential to direct cellular plasticity, specifically differentiate monocytes into M2 macrophages *in vitro* when cultured in inflammation mimicry media. Recently, further investigation by Dinender's group suggested the potential immunomodulation role of BMP-7 by increasing M2 macrophage differentiation and reducing inflammation and plaque formation in Apo $E^{-/-}$ mice [27]. However, up to now, few studies have been performed on potential role of BMP-2 in directing immunoresponse, especially macrophage polarization profiles *in vivo*.

Moreover, pharmacological modulation of inflammatory responses has emerged as a prominent research focus in regenerative medicine [28]. Studies by Ratanavaraporn et al. emphasized that precise regulation of inflammatory pathways serves as a critical determinant for optimizing BMP-2-mediated tissue repair processes [29]. Notably, certain bioactive compounds including agents like dexamethasone (DEX) and heparin demonstrate significant therapeutic potential through their immunomodulatory properties, as evidenced by improved regenerative outcomes in preclinical models [30-33].

The aim of this research is to systematically analyze macrophage activation dynamics during soft-tissue inflammation induced by rhBMP-2-incorporated biomaterial implantation. Given the pivotal role of macrophage-mediated responses in orchestrating tissue regeneration processes [29], our investigation specifically characterizes the phenotypic evolution of macrophages through comprehensive in vivo assessments. This includes evaluation of polarization patterns, quantitative analysis of cytokine release and its gene expression profiles, and histological validation.

Key findings reveal a dose-related macrophage polarization pattern following rhBMP-2 administration, with coexisting M1/M2 subpopulations exhibiting paradoxical pro-inflammatory and

regenerative properties. Significantly, we demonstrate the therapeutic potential of dexamethasone co-delivery in modulating this dual-phase macrophage response. The experimental framework combines controlled animal models with advanced molecular characterization techniques to establish correlations between growth factor dosage, immune cell behavior, and clinical inflammation outcomes.

Materials and methods

Preparation of the rhBMP-2 loaded implants with or without dexamethasone

The commercially available clinical-grade absorbable gelatin sponges utilized in this study were procured from Xiangen Medical Technology Development Co., Ltd. (Jiangxi, China). These sponges were aseptically sectioned into cubic specimens (5 mm × 5 mm × 5 mm) under sterile conditions, followed by 24-hour ultraviolet light sterilization prior to rhBMP-2 loading. Recombinant human BMP-2 (rhBMP-2; molecular weight 26 kDa, concentration 1 mg/mL) was kindly provided by Shanghai Rebone Biomaterials Co., Ltd. (Shanghai, China). Through sterile techniques, varying quantities of rhBMP-2 (with or without dexamethasone) were applied onto the gelatin sponges. After 4 hours incubation for complete absorption, the loaded sponges underwent lyophilization and subsequent storage at 4°C until experimental use.

Animal model and implantation surgery

Four experimental groups were used in this *in vivo* study. All experimental protocols were approved by the Bioethics Committee of East China University of Science and Technology (Shanghai, China. approval number: ECUST-2022-053). All surgical procedures and methods were carried out in accordance with relevant guidelines and regulations. All animal housing and experiments were conducted in strict accordance with the institutional guidelines for care and use of laboratory animals. Animals were anesthetized and sacrificed using acceptable methods/techniques.

Sixty 8-week-old BALB/c mice (Slac Laboratory Animal Co., Ltd. Shanghai, China) with an average weight of 25 g were equally divided into 4 groups: absorbable gelatin sponges without rhBMP-2 (blank control); absorbable gelatin sponges with lower -dose of rhBMP-2 (20 μg, LBMP); absorbable gelatin sponges with higher-dose of rhBMP-2 (50 μg, HBMP); and absorbable gelatin sponges with higher-dose of rhBMP-2 (50 μg) along with 40 μg dexamethasone (HBMP+Dex) respectively. The dosage of dexamethasone sodium phosphate (5 mg/mL injectable formulation; Chengshi Pharmaceutical Co., Ltd., Anhui, China) administered in this experiment was determined based on the conversion table provided in Medical Laboratory Animal Science.

The surgical procedure was performed under strict sterile conditions to establish a subcutaneous implantation model. Mice underwent anesthesia through intraperitoneal injection of 1% pentobarbital sodium (Juli Biotechnology Co., Ltd., Shanghai, China; 60 mg/kg, 0.15 mL per mouse). Following dorsal hair removal and disinfection with 75% medical ethanol, a 1 cm longitudinal incision was created along the midline. A subcutaneous cavity was carefully prepared through blunt dissection, into which a single sponge impregnated with varying doses of rhBMP-2 (with or without dexamethasone) was implanted. The surgical site received layered closure followed by secondary sterilization. Each experimental group comprised 15 animals (n = 15).

Inflammatory exudates and explants

Exudates and explants were collected from the dorsal subcutaneous implantation sites of mice at scheduled time intervals (2, 4, and 7 days post-operation; n = 5). The scientific objectives of the study were successfully achieved, and no further experimentation was required. Mice were then placed in a euthanasia chamber, and CO_2 was introduced at a controlled flow rate (30-70% chamber volume per minute). The flow rate was adjusted using a calibrated control system (50% volume flow = 6.8 L/min). Death was confirmed after 5 minutes by verifying the absence of breathing, rigidity, pupil dilation, and loss of skin color. Throughout the study, experienced personnel conducted daily monitoring were carried out to assess clinical indicators of distress, including altered posture, unkempt fur, ocular/nasal discharge, reduced mobility, or changes in feeding behavior. No adverse clinical signs were observed in

Table 1. Primer pairs used in the real-time PCR

Genes	Sequence
GAPDH	Forward: 5'-GTCGTGGAGTCTACTGGTGTC-3'
	Reverse: 5'-GAGCCCTTCCACAATGCCAAA-3'
IL-1β	Forward: 5'-TGGAGAGTGTGGATCCCAAG-3'
	Reverse: 5'-GGTGCTGATGTACCAGTTGG-3'
IL-6	Forward: 5'-ATAGTCCTTCCTACCCCAATTTCC-3'
	Reverse: 5'-GATGAATTGGATGGTCTTGGTCC-3'
TNF-α	Forward: 5'-CTGAACTTCGGGGTGATCGG-3'
	Reverse: 5'-GGCTTGTCACTCGAATTTTGAGA-3'
IL-10	Forward: 5'-GAGAAGCATGGCCCAGAAATC-3'
	Reverse: 5'-GAGAAATCGATGACAGCGCC-3'
VEGF-A	Forward: 5'-GTCCCATGAAGTGATCAAGTTC-3'
	Reverse: 5'-TCTGCATGGTGATGTTGCTCTCTG-3'

Abbreviations: GAPDH, glyceraldehyde-3-phosphate dehydrogenase; IL-1β, interleukin-1β; IL-6, interleukin-6; TNF-α, tumor necrosis factor-α; IL-10, interleukin-10; VEGF-A, vascular endothelial growth factor-A.

any subjects, confirming compliance with ethical standards.

The surgical sutures were carefully excised and the wound margins were gently separated to minimize tissue trauma. Inflammatory exudates were collected by irrigating the subcutaneous cavities containing sponge implants with 2 mL of phosphate-buffered saline (PBS), followed by aspiration of the lavage fluid. Collected exudates underwent immediate flow cytometric characterization to quantify cellular components. Supernatant fractions were cryopreserved at -80°C to maintain biomolecular stability for subsequent cytokine profiling using enzyme-linked immunosorbent assay (ELISA).

The explantation of implants was conducted immediately following collection of inflammatory exudates. The harvested implants were divided into two processing streams: two explants from each experimental group underwent fixation with 4% paraformaldehyde in PBS to perform subsequent histological and immunofluorescence analyses, while the remaining specimens were cryopreserved in liquid nitrogen for real-time polymerase chain reaction (PCR) investigations.

Flow cytometry

Cell concentration of the exudates were measured by flow cytometer (Accuri C6, BD Bioscience, New York, USA) immediately after the lavage fluid recovery. Fluorescence was detected using FACSAria flow cytometer (BD Biosciense, New York, USA) with Cell Quest software. 10000 events were collected per sample. Analysis was then performed using FlowJo software. All related reagents were purchased from Biolegend (CA, USA).

Real-time polymerase chain reaction (real-time PCR) analysis

The macrophage polarization related cytokine's gene expression was assayed using real-time PCR (qRT-PCR) system (Bio-Rad, Hercules, CA, USA) at 2, 4 and 7 days after implantation. Total RNA of the cells adherent to the implanted sponges was extracted using RNAiso Plus (Takara, Tokyo, Japan) according to the manufacturer's instructions. First-strand cDNA was synthesized with PrimeScript RT reagent Kit (Takara, Tokyo, Japan). Subsequently, cDNA was subjected to real-time PCR using SYBR Premix Ex TaqTM. The qRT PCR was performed as follows: 95°C for 30 s followed by 40 cycles at 95°C for 5 s and 60°C for 34 s. Related markers, including IL-1β, IL-6, TNF-α, IL-10 and VEGF-a were analyzed with glyceraldehyde 3-phosphate dehydrogenase (GAPDH) as the house keeping gene for normalization. The forward and reverse primer sequences used in this study were designed based on cDNA sequences from the NCBI sequence database listed in **Table 1**. All experiments were run in triplicate for each sample and the relative gene expression was expressed as mean ± SD.

Cytokine production

Concentrations of cytokines in inflammatory exudates, including IL-1β, TNF-α, and vascular endothelial growth factor-A (VEGF-A), were determined using enzyme-linked immunosorbent assay (ELISA) kits (Affymetrix eBioscience, CA, USA) following the manufacturer's instructions. Cytokine concentrations were obtained by correlation with a standard calibration curve, and normalized for the total number of cells presented in the corresponding inflammatory exudates.

Histological and immunofluorescence staining evaluation

Following fixation in 4% neutral-buffered paraformaldehyde, the sponge explants were dis-

sected, half of the specimens underwent dehydration through a graded alcohol series (70-100%) followed by paraffin embedding using standard protocols. These paraffin-embedded samples were sectioned at 5 μm thickness using a rotary microtome, with serial sections stained with hematoxylin and eosin (H&E) for histological evaluation. Images were obtained using a light microscope (Leica, Germany) equipped with a digital camera system.

Another half of the explants were made into frozen sections and subjected to immunofluorescence staining process. Fluorescent images were acquired using a fluorescent microscope (Leica, Germany).

Statistical analysis

All experiments described in this investigation were independently replicated in triplicate. Quantitative data are presented as mean ± standard deviation (SD). Statistical significance was determined through one-way ANOVA with post hoc Tukey's multiple comparison test using Origin software. A probability threshold of $P < 0.05$ was established as the criterion for statistical significance.

Results

Histology

Histological analysis through hematoxylin and eosin (H&E) staining was performed on harvested implants. Representative images of the stained sections are presented in **Figure 1** which revealed substantial cellular recruitment at the implantation site during the early postoperative phase (days 2, 4, and 7), with infiltrating cells predominantly localized to the implant periphery. It can be seen that all three rhBMP-2-containing experimental groups elicited higher cell migration to the implantation site compared to the vehicle control group. Quantitative evaluation further indicated that the higher-dose rhBMP-2 group (HBMP-2) exhibited the most pronounced cellular infiltration with cell counts exceeding those observed in other treatment groups. Notably, co-administration of dexamethasone with higher-dose rhBMP-2 (HBMP-2+Dex) resulted in an attenuation of this cellular response, showing reduction in migrated cell numbers relative to HBMP-2 mono-therapy group.

Flow cytometry

Flow cytometric analysis of inflammatory exudates revealed distinct macrophage populations at the implantation site. Macrophages were identified as $F4/80^+$ populations and further classified into M1/M2 subsets using CCR7 (M1 marker) and CD206 (M2 marker), respectively. Representative flow cytometry dot plots are shown in **Figure 2**. Quantitative analysis demonstrated a dose-related relationship in the proportions of both M1 and M2 macrophages between the LBMP and HBMP groups. Notably, the combination of HBMP with Dex administration demonstrated considerable reduction on the percentages of both macrophage phenotypes at the implantation site compared to HBMP treatment alone.

Immunofluorescence staining evaluation

To evaluate the phenotypic characteristics of adherent macrophages and their inflammatory response to varying doses of recombinant human bone morfogenetic protein-2 (rhBMP-2) with or without dexamethasone (Dex), immunofluorescence staining was performed on explanted sponge implants harvested at designated time points. The excised sponges were stained with fluorescent-conjugated antibodies targeting specific macrophage markers and analyzed using fluorescence microscopy.

The following markers were employed to assess macrophage polarization: F4/80 (pan-macrophage marker); CCR7 (M1 pro-inflammatory macrophage marker); CD206 (M2 anti-inflammatory macrophage marker). Macrophage subpopulations were defined as follows: M1 macrophages: dual staining for $F4/80^+/CCR7^+$; M2 macrophages: dual staining for $F4/80^+/CD206^+$.

As demonstrated in **Figure 3**, all rhBMP-2-loaded sponges exhibited significantly higher numbers of both M1 and M2 macrophages compared to the control group post-implantation. A distinct dose-relevant trend was observed: the higher-dose rhBMP-2 (HBMP) group displayed greater adherent M1 and M2 macrophage populations than the lower-dose rhBMP-2 (LBMP) group and the dexamethasone co-administered group. Representative images illustrate dual-stained cells, with co-localized markers appearing yellow.

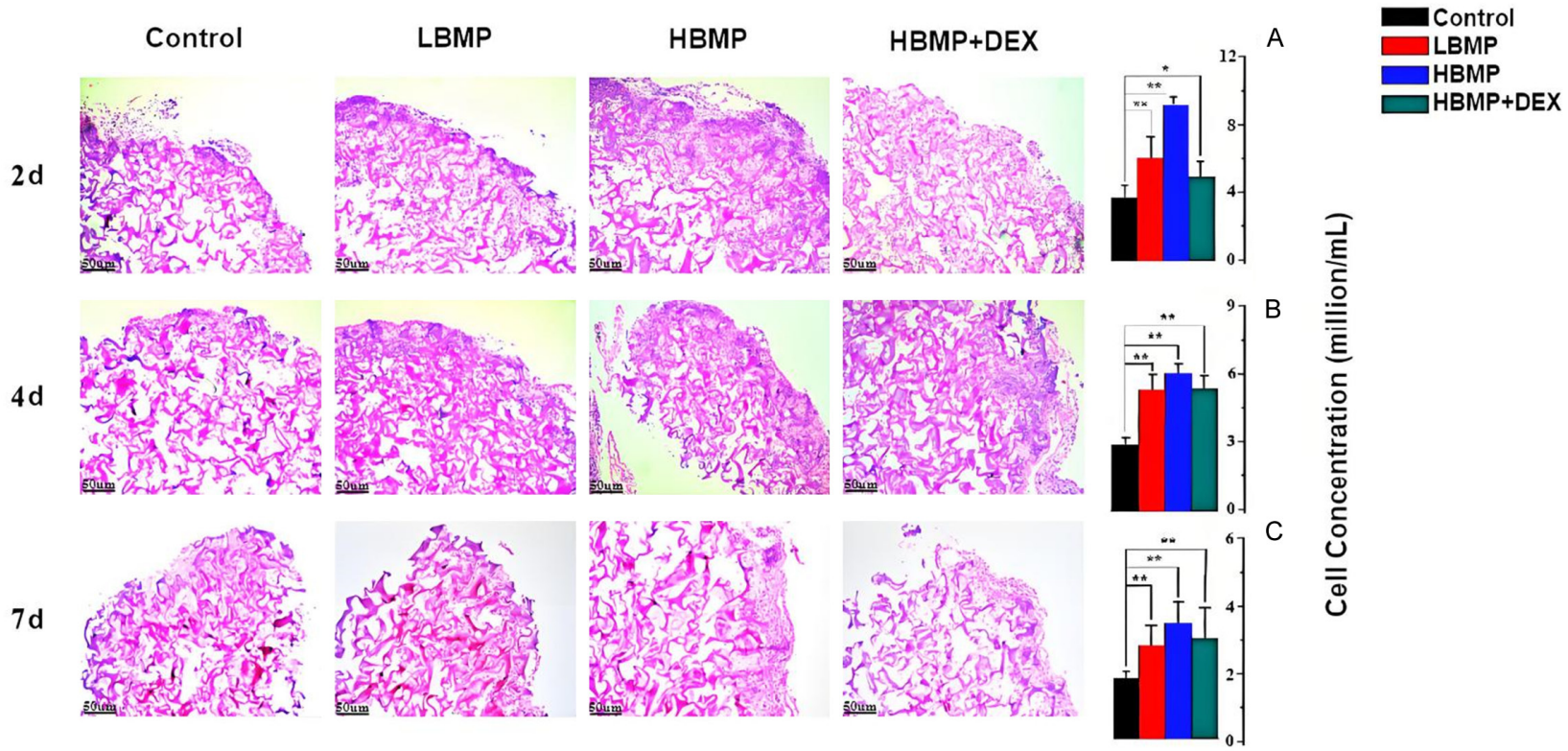

Figure 1. Representative histological images of HE-stained explanted sponges from each experimental group are presented here, clearly indicating the regions colonized with recruited infiltrating cells (Left panel, Scale bar: 50 μm). These images provide a visual representation of cellular infiltration and colonization within the sponges over the course of the experiment. Additionally, a quantitative analysis of cell numbers in the corresponding exudates collected from the mouse dorsal subcutaneous area at 2, 4, and 7 days after implantation is shown (Right panel, A-C). This analysis offers a numerical assessment of the cellular response to the implanted sponges over time.

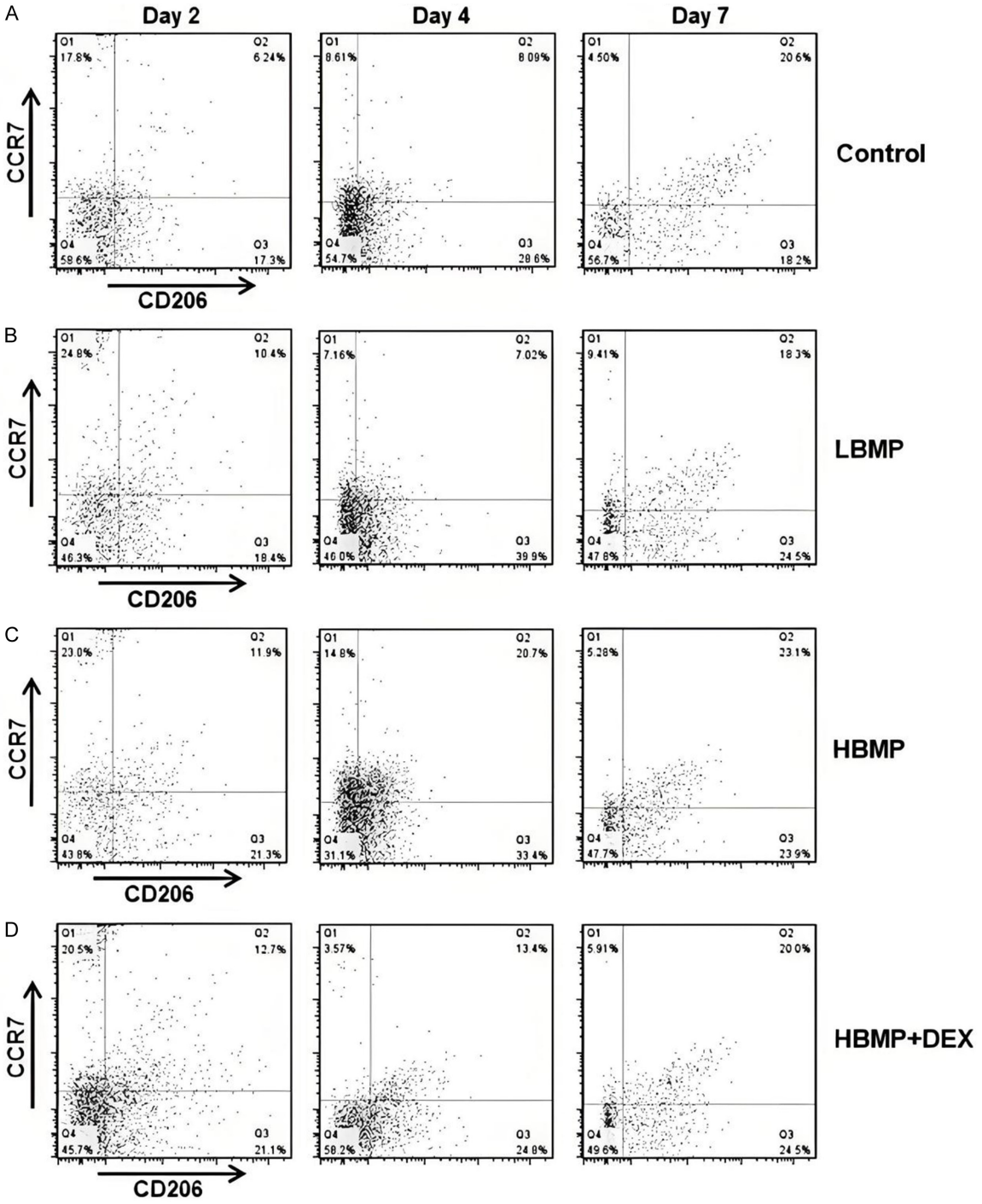

Figure 2. To evaluate the dynamic polarization of macrophages in response to biomaterial implantation, the expression of cell surface markers on macrophages isolated from inflammatory exudates in the mouse dorsal subcutaneous area was analyzed using dual-color immunofluorescence staining for CCR7 (a classical M1 macrophage marker) and CD206 (a prototypical M2 macrophage marker). Representative flow cytometry dot plots are presented, illustrating the co-expression patterns of CCR7 (vertical axis) and CD206 (horizontal axis) antigens across experimental groups. The percentage of F4/80-positive macrophages exhibiting $CCR7^+$ (pro-inflammatory M1 phenotype), $CD206^+$ (anti-inflammatory M2 phenotype), or dual-positive subpopulations was quantified to assess macrophage polarization states under different treatment conditions. A. Control: absorbable gelatin sponges as blank control. B. LBMP: sponges loaded with lower dose rhBMP-2. C. HBMP: sponges loaded with higher dose rhBMP-2. D. HBMP+DEX: sponges loaded with higher dose of rhBMP-2 and Dex.

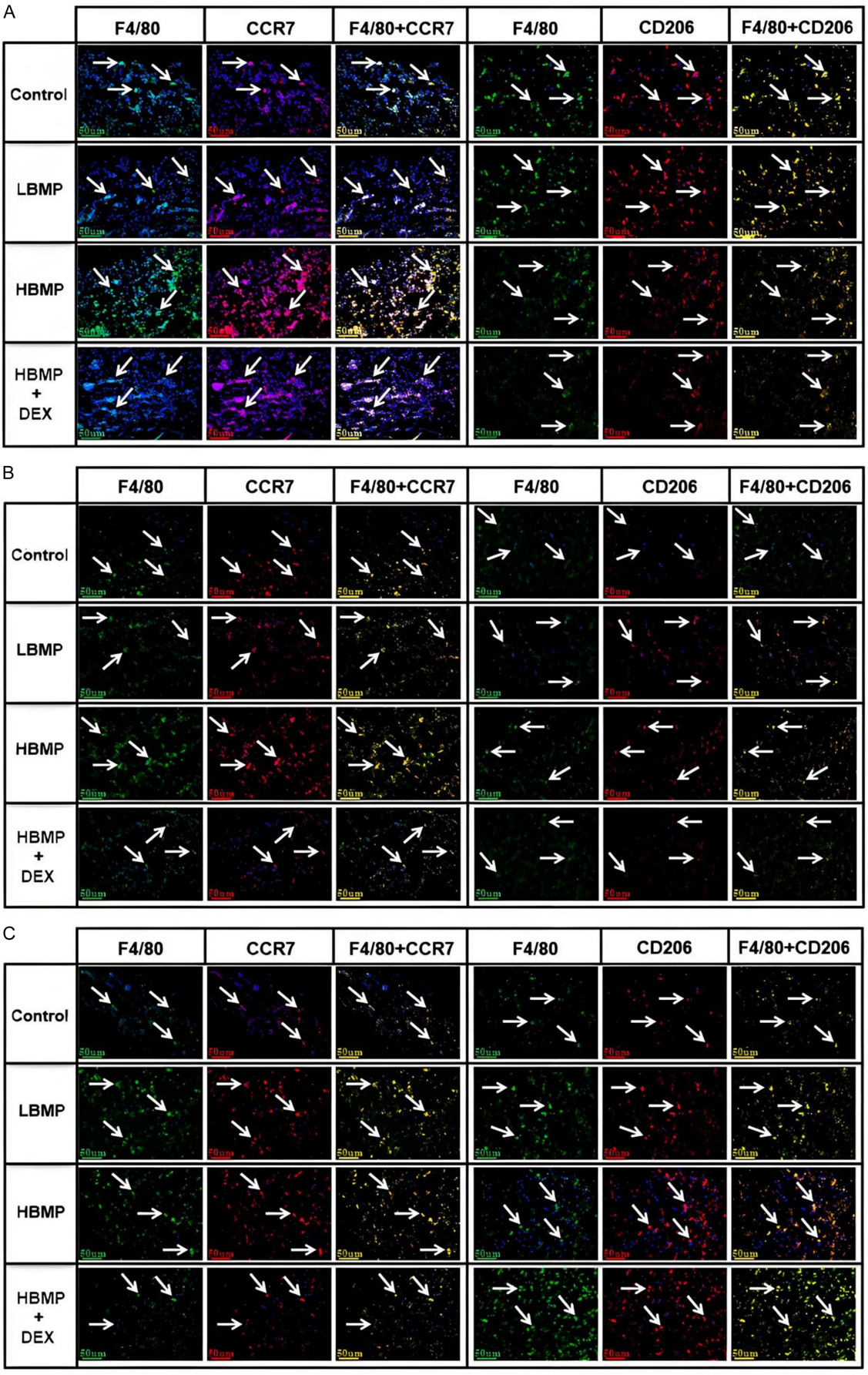
A
F4/80
CCR7
F4/80+CCR7
F4/80
CD206
F4/80+CD206
Control
LBMP
HBMP
HBMP + DEX
B
F4/80
CCR7
F4/80+CCR7
F4/80
CD206
F4/80+CD206
Control
LBMP
HBMP
HBMP + DEX
C
F4/80
CCR7
F4/80+CCR7
F4/80
CD206
F4/80+CD206
Control
LBMP
HBMP
HBMP + DEX

Figure 3. Representative immunofluorescent images of the explanted absorbable gelatin sponges, both with and without the addition of rhBMP-2 and dexamethasone, were captured at 2, 4, and 7 days post-implantation (A-C). In these images, F4/80-positive cells are stained with a green fluorophore, indicating the presence of macrophages. CCR7-positive cells are stained with a red fluorophore, while CD206-positive cells are also stained with a red fluorophore, distinguishing between different macrophage subpopulations. The nuclei of the cells are revealed by DAPI staining, which appears blue. The arrows in the images point out examples of cells that exhibit double staining: F4/80+/CCR7+ cells (appearing yellow) represent M1 macrophages, which are typically pro-inflammatory. Conversely, F4/80+/CD206+ cells (also appearing yellow) represent M2 macrophages, which are generally anti-inflammatory and involved in tissue repair and healing (Scale bar: 50 μm).

Real-time polymerase chain reaction (RT-qPCR) analysis

As illustrated in **Figure 4A-E**, higher-dose bone morphogenetic protein (HBMP) significantly upregulated gene expression levels of pro-inflammatory cytokines (IL-1β, IL-6, TNF-α), anti-inflammatory cytokine IL-10, and pro-angiogenic factor VEGF-a compared to lower-dose BMP (LBMP). Co-administration of dexamethasone (Dex) with HBMP exhibited differential modulation: while substantially suppressing HBMP-induced expression of pro-inflammatory cytokines, it concurrently enhanced the expression levels of IL-10 and VEGF-A relative to HBMP treatment alone.

The experimental data revealed a dose-dependent relationship in rhBMP-2's immunomodulatory effects. Both low and high concentrations stimulated dual-phase cytokine expression profiles characteristic of macrophage polarization. Lower doses predominantly activating M2-type anti-inflammatory responses, whereas higher doses elicited stronger M1-type pro-inflammatory reactions. Notably, Dex demonstrated selective temporal regulation during early inflammatory phases, effectively attenuating HBMP driven pro-inflammatory cytokine expression without compromising the upregulation of anti-inflammatory mediators or angiogenic factors.

This bimodal regulation suggests that HBMP's immunogenic potential can be pharmacologically modulated through glucocorticoid intervention, maintaining its pro-angiogenic benefits while mitigating undesirable inflammatory responses.

Cytokine production

Cytokine profiling of inflammatory exudates harvested from murine dorsal subcutaneous implants revealed distinct macrophage polarization patterns mediated by rhBMP-2 dosage (**Figure 5**). Quantitative analysis demonstrated significant elevation of M1 macrophage-associated pro-inflammatory cytokines (IL-1β, TNF-α) in rhBMP-2-treated groups versus blank controls ($P < 0.05$). Meanwhile, a dose-related escalation was particularly evident between LBMP and HBMP groups; higher dose amplified both M1 and M2 associated pro-inflammatory anti-inflammatory response compared to the lower dose. Statistically significant differences were observed for IL-1β at day 2 and TNF-α at days 2 and 4 and VEGF-A at 4 and 7 days post-implantation. This biphasic regulation suggests rhBMP-2 simultaneously induce inflammatory initiation through M1 activation and tissue remodeling via M2-mediated angiogenesis.

Dexamethasone co-administration exerted selective immunomodulatory effects so that it attenuated IL-1β and TNF-α levels versus HBMP alone at early-phase time-points. Conversely, the M2-associated pro-angiogenic factor VEGF-A was maintained or increased.

Discussion

In this investigation, we systematically examined the dynamic polarization patterns of macrophages in a murine dorsal subcutaneous model following implantation of absorbable gelatin sponges incorporating graded concentrations of recombinant human bone morphogenetic protein-2 (rhBMP-2). The therapeutic potential of concurrent dexamethasone administration was concurrently evaluated. Our experimental data revealed that biomaterial-mediated rhBMP-2 delivery induces simultaneous activation of both pro-inflammatory M1 and reparative M2 macrophage phenotypes. Quantitative analysis demonstrated a biphasic immune response characterized by an exudative phase followed by substantial macrophage infiltration. Notably, the inflammatory cascade exhibited concurrent upregulation of both

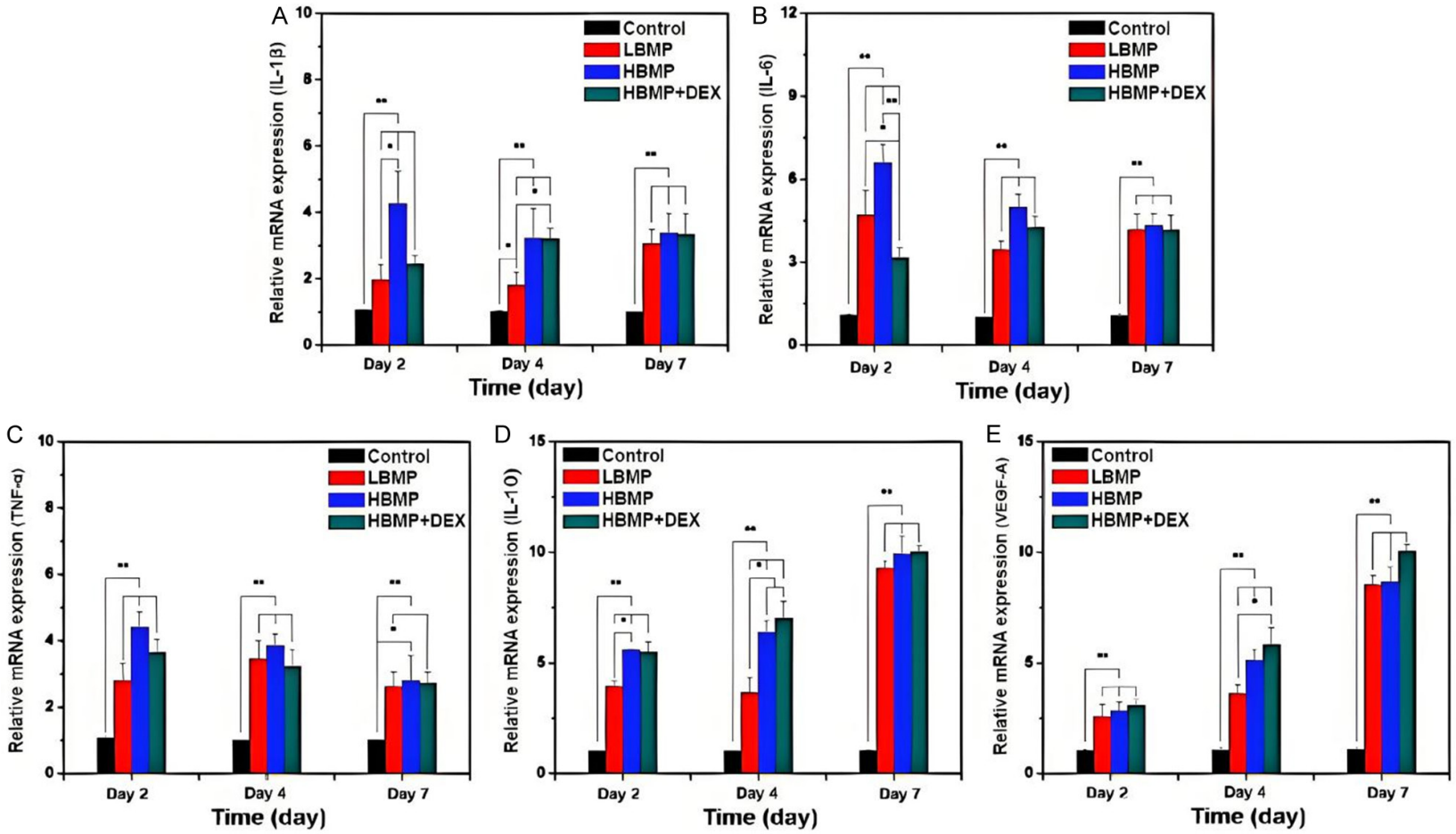

Figure 4. Gene expression profiles of pro-inflammatory cytokines interleukin-1β (IL-1β), interleukin-6 (IL-6), tumor necrosis factor-α (TNF-α) and anti-inflammatory cytokine interleukin-10 (IL-10) along with vascular endothelial growth factor-A (VEGF-A) in inflammatory cells colonizing explanted sponges were quantitatively analyzed across experimental groups using real-time PCR. Statistically significant differences between groups are denoted as *P < 0.05 and **P < 0.01. A. IL-1β expression levels. B. IL-6 expression levels. C. TNF-α expression levels. D. IL-10 expression levels. E. VEGF-A expression levels.

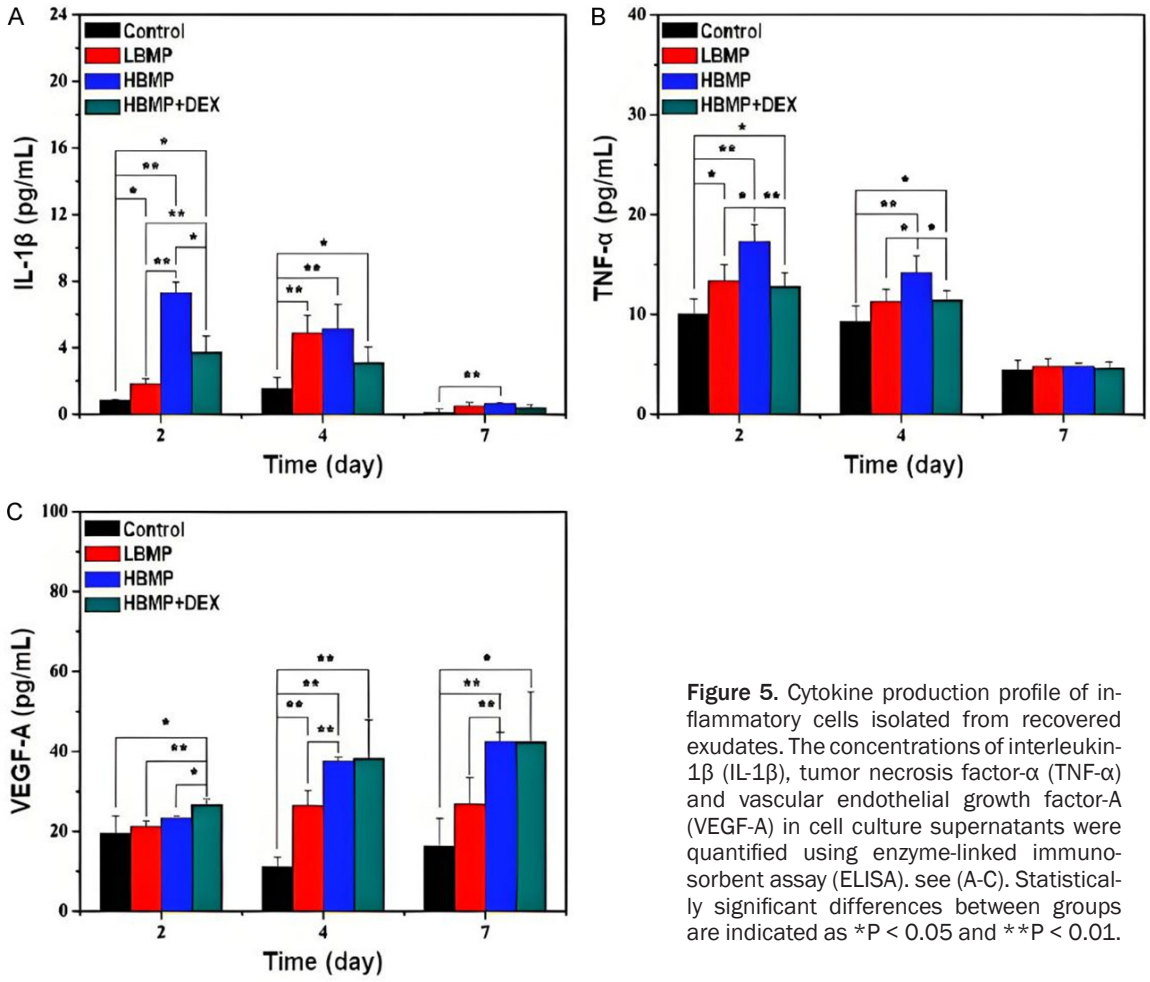

Figure 5. Cytokine production profile of inflammatory cells isolated from recovered exudates. The concentrations of interleukin-1β (IL-1β), tumor necrosis factor-α (TNF-α) and vascular endothelial growth factor-A (VEGF-A) in cell culture supernatants were quantified using enzyme-linked immunosorbent assay (ELISA). see (A-C). Statistically significant differences between groups are indicated as *P < 0.05 and **P < 0.01.

M1-associated pro-inflammatory markers and M2-related anti-inflammatory mediators, suggesting a complex immunomodulatory interaction between the host tissue and growth factor-loaded scaffold.

Comprehensive analysis of macrophage polarization dynamics demonstrated that rhBMP-2 implantation elicited dual activation of both M1 and M2 subpopulations in vivo. Phenotypic profiling through lineage-specific surface markers revealed significantly elevated proportions of F4/80+CCR7+ (M1) and F4/80+CD206+ (M2) cells in rhBMP-2-treated inflammatory exudates compared to baseline controls, with observed dose-dependent amplification of both activation states (**Figure 2**). This bimodal macrophage activation pattern corroborates emerging paradigms in regenerative medicine, as evidenced by Mokarram et al.'s seminal work proposing that tissue repair outcomes are principally governed by the functional polarization states of infiltrating macrophages rather than mere cellular abundance at injury sites [34]. The current findings further substantiate the critical role of microenvironmental cytokine milieus in directing macrophage phenotypic commitments during biomaterial-mediated osteogenesis.

As an exogenous growth factor, HBMP demonstrated a dose-related tendency to trigger more pronounced inflammatory reactions and cellular activation compared to LBMP. These observations were further supported by quantitative analyses of cytokine concentrations in inflammatory exudates and transcriptional profiling of immune cells localized at implantation sites. As depicted in **Figure 6**, rhBMP-2-loaded implants exhibited elevated levels of both pro-inflammatory mediators (IL-1β, TNF-α) and pro-angiogenic signaling molecules (VEGF-A), reflecting characteristic biomarkers of sequential M1/M2 macrophage polarization. This cytokine induc-

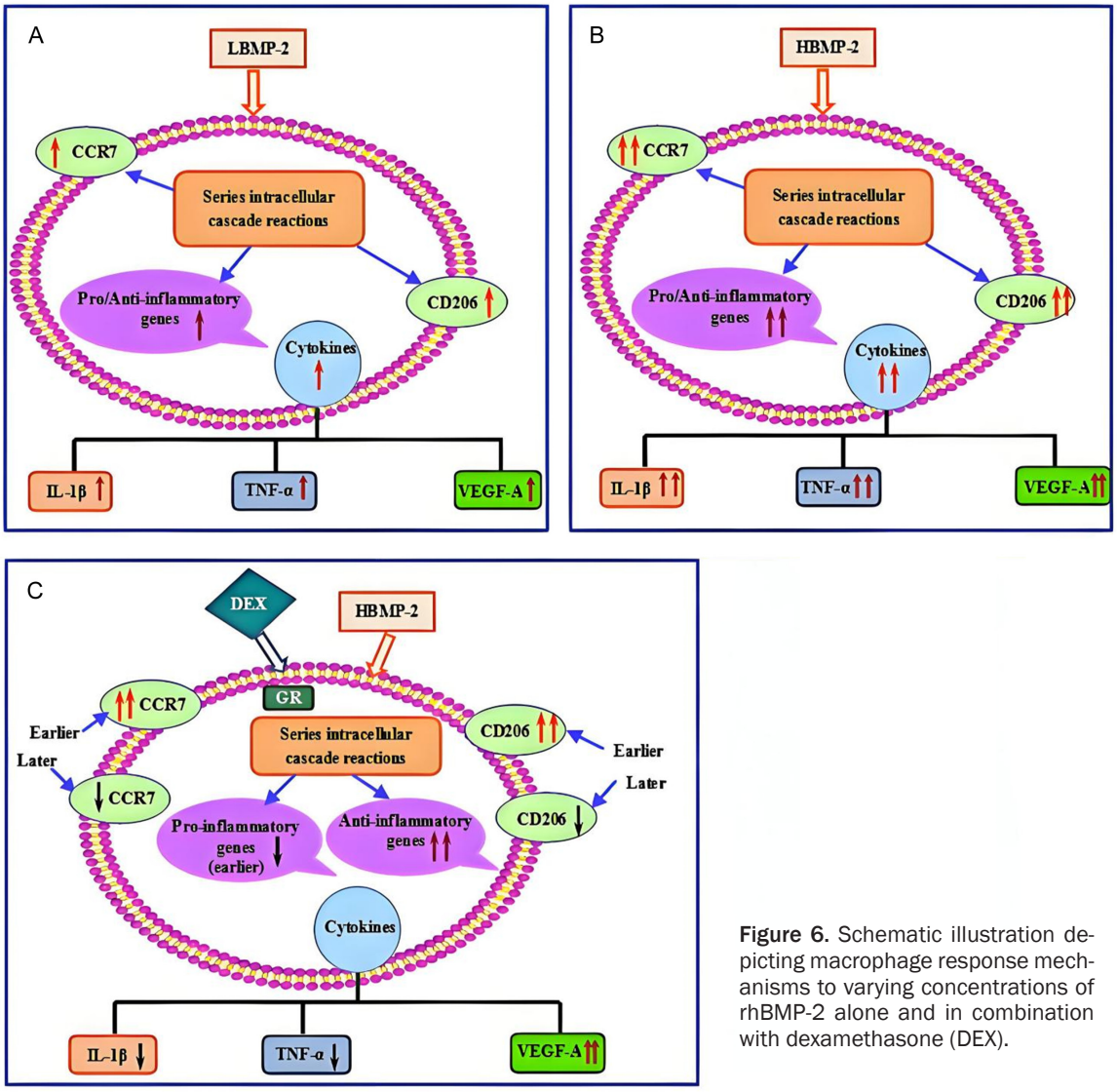

Figure 6. Schematic illustration depicting macrophage response mechanisms to varying concentrations of rhBMP-2 alone and in combination with dexamethasone (DEX).

tion pattern showed clear concentration dependence, as evidenced by the graded response illustrated in **Figure 5**. Parallel transcriptional analyses revealed analogous dose-responsive regulation, with rhBMP-2 treatment groups displaying significant upregulation of both pro-inflammatory genes (IL-1β, IL-6, TNF-α) and anti-inflammatory mediator (IL-10), alongside enhanced VEGF-A expression (**Figure 4**). Notably, the maximal induction of anti-inflammatory cytokines appeared proportional to the magnitude of pro-inflammatory signaling, suggesting a compensatory regulatory mechanism to modulate excessive immune activation. These molecular findings align with prior flow cytometry data documenting rhBMP-2's dose-dependent influence on macrophage differentiation dynamics within inflammatory exudates.

Histopathological and immunohistochemical analyses substantiated distinct cellular distribution patterns between experimental groups, particularly in adherent cell density at the implantation site and macrophage phenotypic marker expression. Hematoxylin-eosin (H&E) staining results (**Figure 1**) revealed predominant inflammatory cell aggregation along the peripheral regions of implants, with higher-dose BMP (HBMP) demonstrating consistently elevated inflammatory cell recruitment across all observation periods compared to lower-dose BMP (LBMP). This spatial distribution pattern was corroborated by immunofluorescence find-

ings (**Figure 3**), where rhBMP-2 supplemented groups exhibited dose-dependent augmentation of both M1 and M2 macrophage populations relative to controls.

As a prototypical glucocorticoid receptor agonist with potent anti-inflammatory properties, dexamethasone was strategically co-administered with high-concentration rhBMP-2 formulations in this investigation [35]. This combinatorial approach effectively counteracted rhBMP-2-induced pro-inflammatory cytokine secretion (**Figures 4**, **5**) while preserving the therapeutic agent's capacity to stimulate anti-inflammatory cytokine production. Histopathological evaluation further demonstrated significant attenuation of inflammatory cell infiltration at implantation sites (**Figure 1**), establishing a concordance between cytokine modulation and cellular response patterns.

Our findings collectively indicate that inflammatory responses induced by rhBMP-2 administration exhibit dose-related amplification during the early inflammatory phase. The experimental data reveal a dual regulatory mechanism where varying concentrations of rhBMP-2 differentially modulate macrophage polarization, promoting both pro-inflammatory (M1, F4/80+CCR7+) and anti-inflammatory (M2, F4/80+CD206+) phenotypes. Specifically, elevated rhBMP-2 concentrations demonstrated three distinct dose-response relationships: (1) Enhanced cellular infiltration with increased macrophage recruitment and adhesion at implantation sites. (2) Proportional elevation in both M1 and M2 macrophage subpopulations. (3) Concurrent upregulation of pro-inflammatory cytokines (IL-1β, TNF-α), anti-inflammatory mediator IL-10 and growth factor (VEGF-A) expression. This dose-related immunomodulatory pattern corroborates clinical observations regarding rhBMP-2-related complications, particularly the dose-associated incidence of soft tissue inflammation and postoperative edema documented in prior studies [25]. The biphasic cytokine activation mechanism identified in our research provides a potential molecular basis for these clinical phenomena.

Furthermore, our findings revealed that the combined application of dexamethasone and higher-dose rhBMP-2-loaded biomaterials resulted in three distinct biological advantages compared to higher-dose rhBMP-2 monotherapy: 1) significant reduction in macrophage infiltration (particularly M1 macrophages [F4/80+CCR7+]), 2) downregulation of pro-inflammatory cytokine production at both transcriptional and secretory levels, while 3) maintaining elevated expression of pro-angiogenic growth factors (**Figures 1**-**5**). This synergistic regimen demonstrated dexamethasone's remarkable capacity to modulate macrophage dynamics - including migratory patterns, tissue distribution and polarization states within the inflammatory microenvironment induced by rhBMP-2.

Although this combination strategy may not represent the optimal approach for comprehensive immunomodulation, it provides a clinically relevant alternative for mitigating rhBMP-2 dose-related inflammatory complications. The therapeutic significance lies in its ability to preserve rhBMP-2's osteoinductive benefits while effectively counteracting its pro-inflammatory side effects, particularly in clinical scenarios where higher-dose rhBMP-2 administration remains necessary but requires adverse reaction management.

To our current understanding, this represents a pioneering in vivo investigation evaluating dose-related modulation of macrophage polarization dynamics post-implantation of rhBMP-2 functionalized biomaterials. Our experimental data revealed significant variations in macrophage recruitment patterns, phenotypic transformation trajectories, and associated cytokine gene regulatory networks across different rhBMP-2 concentration gradients. Notably, biomaterial carriers incorporating rhBMP-2 induced simultaneous activation of both M1 and M2 polarization pathways, demonstrating the inherent cellular plasticity that enables phenotypic inter-conversion between these subsets [36]. This finding aligns with emerging evidence confirming macrophage heterogeneity, where individual cells may co-express canonical M1/M2 surface markers during transitional phases [37]. Crucially, persistent M1-dominant activation was observed to compromise tissue regeneration outcomes through catabolic matrix degradation pathways, potentially exacerbating inflammatory tissue damage [29, 38]. Furthermore, this study systematically investigated the immunomodulatory synergy between combinatorial rhBMP-2 and dexamethasone delivery. Importantly, concurrent administration of

dexamethasone with high-dose rhBMP-2 formulations effectively mitigated foreign body response severity while promoting favorable macrophage polarization profiles conducive to tissue repair.

Conclusion

The inflammatory response induced by recombinant human bone morphogenetic protein-2 (rhBMP-2)-loaded biomaterials exhibits a distinct dose-response relationship. Elevated rhBMP-2 concentrations provoke amplified immunological activation, characterized by enhanced immune cell infiltration and bidirectional macrophage polarization toward both M1 (pro-inflammatory) and M2 (anti-inflammatory) phenotypes. This dual polarization is accompanied by concurrent upregulation of pro-inflammatory cytokines (e.g., IL-1β, TNF-α) and anti-inflammatory mediators (e.g., IL-10, TGF-β), reflecting the paradoxical nature of macrophage responses. Notably, the M1/M2 dichotomy manifests as a therapeutic double-edged sword. While M2 macrophages facilitate tissue repair through regenerative signaling, excessive M1 activation at supraphysiological rhBMP-2 doses precipitates robust inflammation that may induce iatrogenic tissue damage and impede remodeling processes through sustained inflammatory cascades. These findings underscore the critical importance of optimizing rhBMP-2 dosage in clinical applications. Therapeutic windows should be established to maximize osteoinductive efficacy while minimizing inflammatory complications-a crucial consideration for achieving predictable surgical outcomes. In scenarios requiring high-dose rhBMP-2 administration, concomitant use of anti-inflammatory agents (e.g., dexamethasone) through controlled delivery systems warrants investigation to mitigate adverse inflammatory responses without compromising osteogenesis. This dose-stratified approach aligns with current trends in precision biomaterial engineering and combination therapy development for bone regeneration.

Acknowledgements

We appreciate the support from the National Natural Science Foundation of China for Innovative Research Groups (No. 51621002) and the National Natural Science Foundation of China (No. 31870953).

Disclosure of conflict of interest

None

Address correspondence to: Jing Wang, The State Key Laboratory of Bioreactor Engineering, East China University of Science and Technology, 130 Meilong Road, Shanghai 200237, China. E-mail: 402560495@qq.com; wjbiomat@163.com

References

[1] Rundle CH, Wang H, Yu H, Chadwick RB, Davis EI, Wergedal JE, Lao KH, Mohan S, Ryaby JT and Bylink DJ. Microarray analysis of gene expression during the inflammation and endochondral bone formation stages of rat femur fracture repair. Bone 2006; 38: 521-529.

[2] Sun JL, Jiao K, Niu LN, Jiao Y, Song Q, Shen LJ, Tay FR and Chen JH. Intrafibrillar silicified collagen scaffold modulates monocyte to promote cell homing, angiogenesis and bone regeneration. Biomaterials 2017; 113: 203-216.

[3] Cooper PR, Takahashi Y, Graham LW, Simon S, Imazato S and Smith AJ. Inflammation-regeneration interplay in the dentine-pulp complex. J Dent 2010; 38: 687-697.

[4] Goertz O, Ring A, Buschhaus B, Hirsch T, Daigeler A, Steinstraesser L, Steinau HU and Langer S. Influence of anti-inflammatory and vasoactive drugs on microcirculation and angiogenesis after burn in mice. Burns 2011; 37: 656-664.

[5] Corsetti G, Antona GD, Dioguardi FS and Rezzani R. Topical application of dressing with amino acids improves cutaneous wound healing in aged rats. Acta Histochem 2010; 112: 497-507.

[6] Loeffler J, Duda GN, Sass FA and Dienelt A. The metabolic microenvironment steers bone tissue regeneration. Trends Endocrinol Metab 2018; 29: 99-110.

[7] Anderson JM, Rodriguez A and Chang DT. Foreign body reaction to biomaterials. Semin Immunol 2008; 20: 86-100.

[8] Blakney AK, Swartzlander MD and Bryant SJ. The effects of substrate stiffness on the in vitro activation of macrophages and in vivo host response to poly(ethyleneglycol)-based hydrogels. J Biomed Mater Res A 2012; 100: 1375-1386.

[9] Bartneck M, Heffels KH, Pan Y, Bovi M, Zwadlo-Klarwasser G and Groll J. Inducing healing-like human primary macrophage phenotypes by 3D hydrogel coated nanofibres. Biomaterials 2012; 33: 4136-4146.

[10] Schutte RJ, Parisi-Amon A and Reichert WM. Cytokine profiling using monocytes/macro-

phages cultured on common biomaterials with a range of surface chemistries. J Biomed Mater Res A 2008; 88: 128-139.
[11] Ji J, Hu SL, Cui ZW and Li WF. Probiotic bacillus amyloliquefaciens mediate M1 macrophage polarization in mouse bone marrow-derived macrophages. Arch Microbiol 2013; 195: 349-356.
[12] Garlet GP and Giannobile WV. Macrophages: the bridge between inflammation resolution and tissue repair? J Dent Res 2018; 97: 1079-1081.
[13] Ma QL, Fang L, Jiang N, Zhang L, Wang Y, Zhang YM and Chen LH. Bone mesenchymal stem cell secretion of sRANKL/OPG/M-CSF in response to macrophage-mediated inflammatory response influences osteogenesis on nanostructured Ti surfaces. Biomaterials 2018; 154: 234-247.
[14] Garaicoa-Pazmino C, Fretwurst T, Squarize CH, Berglundh T, Giannobile WV, Larsson L and Castilho RM. Characterization of macrophage polarization in periodontal disease. J Clin Periodontol 2019; 46: 830-839.
[15] Yu T, Zhao L, Huang X, Ma C, Wang Y, Zhang J and Xuan D. Enhanced activity of the macrophage M1/M2 phenotypes and phenotypic switch to M1 in periodontal infection. J Periodontol 2016; 87: 1092-1102.
[16] Jin SS, He DQ, Luo D, Wang Y, Yu M, Guan B, Fu Y, Li ZX, Zhang T, Zhou YH, Wang CY and Liu Y. A biomimetic hierarchical nanointerface orchestrates macrophage polarization and mesenchymal stem cell recruitment to promote endogenous bone regeneration. ACS Nano 2019; 13: 6581-6595.
[17] Genin M, Clement F, Fattaccioli A, Raes M and Michiels C. M1 and M2 macrophages derived from THP-1 cells differentially modulate the response of cancer cells to etoposide. BMC Cancer 2015; 15: 577.
[18] Mahon OR, Browe DC, Gonzalez-Fernandez T, Pitacco P, Whelan IT, Von Euw S, Hobbs C, Nicolosi V, Cunningham KT, Mills KHG, Kelly DJ and Dunne A. Nano-particle mediated M2 macrophage polarization enhances bone formation and MSC osteogenesis in an IL-10 dependent manner. Biomaterials 2020; 239: 119833.
[19] Zhuang Z, Yoshizawa-Smith S, Glowacki A, Maltos K, Pacheco C, Shehabeldin M, Mulkeen M, Myers N, Chong R, Verdelis K, Garlet GP, Little S and Sfeir C. Induction of M2 macrophages prevents bone loss in murine periodontitis models. J Dent Res 2019; 98: 200-208.
[20] Mantovani A, Sica A and Locati M. Macrophage polarization comes of age. Immunity 2005; 23: 344-346.
[21] Banchereau J, Pascual V and O'Garra A. From IL-2 to IL-37: the expanding spectrum of anti-inflammatory cytokines. Nat Immunol 2012; 13: 925-931.
[22] Troidl C, Jung G, Troidl K, Hoffmann J, Mollmann H, Nef H, Schaper W, Hamm CV and Schmitz-Rixen T. The temporal and spatial distribution of macrophage subpopulations during arteriogenesis. Curr Vasc Pharmacol 2013; 11: 5-12.
[23] Shields LB, Raque GH, Glassman SD, Campbell M and Vitaz T. Adverse effects associated with high-dose recombinant human bone morphogenetic protein-2 use in anterior cervical spine fusion. Spine 2006; 31: 542-547.
[24] James AW, LaChaud G, Shen J, Asatrian G, Nguyen V, Zhang X, Ting K and Soo C. A review of the clinical side effects of bone morphogenetic protein-2. Tissue Eng Part B Rev 2016; 22: 284-297.
[25] Lee KB, Taghavi CE, Murray SS, Song KJ, Keorochana G and Wang JC. BMP induced inflammation: a comparison of rhBMP-7 and rhBMP-2. J Orthop Res 2012; 30: 1985-1994.
[26] Rocher C and Singla DK. SMAD-PI3K-Akt-mTOR pathway mediates BMP-7 polarization of monocytes into M2 macrophages. PLoS One 2013; 8: e84009.
[27] Singla DK, Singla R and Wang J. BMP-7 treatment increases M2 macrophage differentiation and reduces inflammation and plaque formation in Apo E-/- mice. Plos One 2016; 11: e0147897.
[28] Peng LH, Ko CH, Siu SW, Koon CM, Yue GL, Cheng WH, Lau TW, Han QB, Ng KM, Fung KP, Lau CB and Leung PC. In vitro & in vivo assessment of a herbal formula used topically for bone fracture treatment. J Ethnopharmacol 2010; 131: 282-289.
[29] Ratanavaraporn J, Furuya H and Tabata Y. Local suppression of pro-inflammatory cytokines and the effects in BMP-2-induced bone regeneration. Biomaterials 2012; 33: 304-316.
[30] Spiller KL, Nassiri S, Witherel CE, Anfang RR, Ng J, Nakazawa KR, Yu T and Vunjak-Novakovic G. Sequential delivery of immunomodulatory cytokines to facilitate the M1-to-M2 transition of macrophages and enhance vascularization of bone scaffolds. Biomaterials 2015; 37: 194-207.
[31] Norton LW, Koschwanez HE, Wisniewski NA, Klitzman B and Reichert WM. Vascular endothelial growth factor and dexamethasone release from nonfouling sensor coatings affect the foreign body response. J Biomed Mater Res A 2007; 81: 858-869.
[32] Giulietti A, Etten EV, Overbergh L, Stoffels K, Bouillon R and Mathieu C. Monocytes from type 2 diabetic patients have a pro-inflammatory profile: 1,25-Dihydroxyvitamin D3 works as anti-inflammatory. Diabetes Res Clin Pr 2007; 77: 47-57.

[33] Kim SE, Song SH, Yun YP, Choi BJ, Kwon IK, Bae MS, Moon HJ and Kwon YD. The effect of immobilization of heparin and bone morphogenic protein-2 (BMP-2) to titanium surfaces on inflammation and osteoblast function. Biomaterials 2011; 32: 366-373.

[34] Mokarram N, Merchant A, Mukhatyar V, Patel G and Bellamkonda RV. Effect of modulating macrophage phenotype on peripheral nerve repair. Biomaterials 2012; 33: 8793-8801.

[35] Oelzner P, Fleissner-Richter S, Bräuer R, Hein G, Wolf G and Neumann T. Combination therapy with dexamethasone and osteoprotegerin protects against arthritis-induced bone alterations antigen-induced arthritis of the rat. Inflamm Res 2010; 59: 731-741.

[36] Mooney JE, Rolfe BE, Osborne GW, Sester DP, van Rooijen N, Campbell GR, Hume DA and Campbell JH. Cellular plasticity of inflammatory myeloid cells in the peritoneal foreign body response. Am J Pathol 2010; 176: 369-380.

[37] Pettersen JS, Fuentes-Duculan J, Suárez-Fariñas M, Pierson KC, Pitts-Kiefer A, Fan L, Belkin DA, Wang CQ, Bhuvanendran S, Johnson-Huang LM, Bluth MJ, Krueger JG, Lowes MA and Carucci JA. Tumor-associated macrophages in the cutaneous SCC micro-environment are heterogeneously activated. J Invest Dermatol 2011; 131: 1322-1330.

[38] Zaveri TD, Lewis JS, Dolgova NV, Clare-Salzler MJ and Keselowsky BG. Integrin-directed modulation of macrophage responses to biomaterials. Biomaterials 2014; 35: 3504-3515.